VIP Photocatalysis Very Important Paper

International Edition: DOI: 10.1002/anie.201602973
German Edition: DOI: 10.1002/ange.201602973

Stable Aqueous Photoelectrochemical CO_2 Reduction by a Cu_2O Dark Cathode with Improved Selectivity for Carbonaceous Products

*Xiaoxia Chang[+], Tuo Wang[+], Peng Zhang, Yijia Wei, Jiubing Zhao, and Jinlong Gong**

Abstract: *Photocatalytic reduction of CO_2 to produce fuels is a promising way to reduce CO_2 emission and address the energy crisis. However, the H_2 evolution reaction competes with CO_2 photoreduction, which would lower the overall selectivity for carbonaceous products. Cu_2O has emerged as a promising material for suppressing the H_2 evolution. However, it suffers from poor stability, which is commonly regarded as the result of the electron-induced reduction of Cu_2O. This paper describes a simple strategy using Cu_2O as a dark cathode and TiO_2 as a photoanode to achieve stable aqueous CO_2 reduction with a high Faradaic efficiency of 87.4% and a selectivity of 92.6% for carbonaceous products. We have shown that the photogenerated holes, instead of the electrons, primarily account for the instability of Cu_2O. Therefore, Cu_2O was used as a dark cathode to minimize the adverse effects of holes, by which an improved stability was achieved compared to the Cu_2O photocathode under illumination. Additionally, direct exposure of the Cu_2O surface to the electrolyte was identified as a critical factor for the high selectivity for carbonaceous products.*

The excessive utilization of fossil fuels accompanied with large amounts of CO_2 emissions has led to the global energy and environmental crisis.[1] Photocatalytic (PC) and photoelectrochemical (PEC) reduction of CO_2 into fuels utilizing solar energy could address both problems, and have received increasing attention since the seminal investigation in 1978.[2] However, the photoreduction of CO_2 with H_2O suffers from low Faradaic efficiency (FE) and selectivity for carbonaceous products (denoted as SCP, defined in the Supporting Information) owing to many limiting factors. Thermodynamically, CO_2 is an extremely stable molecule and its activation requires a large energy input.[3] In addition, the thermodynamic equilibrium potentials for CO_2 reduction are very close to that of H_2 evolution reaction (HER), leading to a strong competition between the two reactions (Supporting Information, Table S1).[4] Kinetically, the reduction of CO_2 involves multiple proton-coupled electron transfers, and the associated kinetic barriers in each step must be overcome for the forward reaction.[3] The reduction of H_2O is kinetically more favorable than CO_2 reduction, rendering H_2 as the major product. Thus, the design and fabrication of efficient CO_2 photoreduction systems with high FE and SCP remain a major challenge.[5]

Recently, copper-based materials (metallic Cu, CuO, and Cu_2O) have gained much attention for photocatalysis owing to their low toxicity and high abundance.[6] Lee and co-workers constructed a photoanode-driven PEC system consisting of a WO_3 photoanode and Cu cathode for CO_2 photoreduction. The FE of 71.6% for all of the carbonic products was achieved.[7] In particular, among the copper-based materials, cuprous oxide (Cu_2O) with a direct band gap of $\approx$2.0 eV has emerged as a promising material for promoting CO_2 conversion and suppressing HER in PC and PEC CO_2 reduction.[2b] Rajeshwar and co-workers first reported the utilization of Cu_2O for CO_2 photoreduction. They synthesized hybrid CuO–Cu_2O nanorod arrays (NRs) on Cu substrates and achieved a FE of $\approx$95% for the photoelectrosynthesis of methanol from CO_2 in aqueous solutions.[8] Wang and co-workers prepared a core–shell-structured Pt@Cu_2O cocatalyst on TiO_2 nanoparticles for PC CO_2 reduction in aqueous solutions, and achieved a significant promotion of CH_4 and CO generation. The highest SCP reached up to 85%. They proposed that the Cu_2O shell provided active sites for the preferential conversion of CO_2 molecules and suppressed HER.[9] However, one of the major drawbacks of Cu_2O is its poor stability, which potentially limits its large-scale utilization in photocatalytic reactions. Because the redox potentials for the reduction and oxidation of Cu_2O lie within its band gap, it can be easily corroded in aqueous solutions under illumination, leading to the loss of preferential CO_2 reduction capability and a low SCP.[10] Being commonly used as a cathode, the deactivation of Cu_2O is generally considered to be due to its reduction to Cu caused by electrons.[11] To address this issue, many studies have focused on the coating of suitable protective layers with favorable energy band positions, such as TiO_2, on bare Cu_2O for stable and efficient photoreduction of H_2O or CO_2, instead of the self-reduction of Cu_2O.[10,12] However, the coating of protective layers would cover the active sites for the preferential reduction of CO_2 on the surface of Cu_2O. As a result, a large amount of H_2 will be generated and the SCP will decrease sharply. Grätzel and colleagues also noticed this phenomenon and coupled the TiO_2-protected Cu_2O photoelectrode with a Re(tBu-bipy)$(CO)_3$Cl molecular catalyst to selectively reduce CO_2 molecules instead of H_2O, which improved the stability of Cu_2O and avoided the extensive generation of H_2.[12b,13]

This paper describes a simple strategy using Cu_2O as a dark cathode and TiO_2 as a model photoanode to devise a stable system for PEC CO_2 reduction with high FE and SCP. First, in order to utilize the active reaction sites on Cu_2O for the preferential conversion of CO_2 molecules and the suppression of HER, the surface of Cu_2O was directly exposed into the electrolytes and resulted in a higher SCP than typical Pt/Cu metal cathodes and TiO_2-protected Cu_2O cathodes. Second, back-side illumination was utilized to investigate the deactivation mechanism of Cu_2O, and it was found that the photogenerated holes, instead of electrons, are the major reason for the corrosion of Cu_2O. Therefore, the Cu_2O film was used as a dark cathode to minimize the adverse effects of holes, exhibiting an unexpected and much better stability during the 3 h reaction than that directly used as photocathode under illumination. As a result, a high FE of 87.45% and SCP of 92.65% for all of the carbonaceous products were achieved, which is among the highest SCPs

[*] X. Chang,[+] Dr. T. Wang,[+] Dr. P. Zhang, Y. Wei, J. Zhao, Prof. Dr. J. Gong
Key Laboratory for Green Chemical Technology of Ministry of Education
School of Chemical Engineering and Technology
Tianjin University; Collaborative Innovation Center of Chemical Science and Engineering
Tianjin 300072 (China)
E-mail: jlgong@tju.edu.cn
[+] These authors contributed equally to this work.
Supporting information and the ORCID identification number(s) for the author(s) of this article can be found under http://dx.doi.org/10.1002/anie.201602973.

ever reported for CO_2 photoreduction in aqueous solutions without hole scavengers.[7,9,14]

The Cu_2O electrode was synthesized by an electrodeposition method on Cu substrate and TiO_2 nanorod (NR) photoanode was obtained by a facile hydrothermal method (see the Supporting Information for experimental details).[15] The Cu_2O grains of the film show a cubic morphology and exhibit a predominant (111) orientation, as evidenced by the transmission electron microscopy (TEM), high-resolution TEM (HRTEM), and field-emission scanning electron microscopy (FESEM) images (Figure 1). The high photoactivity

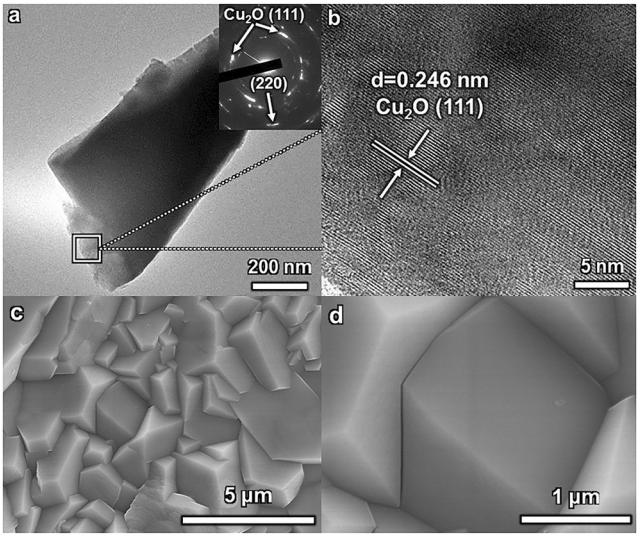

Figure 1. a) TEM, b) HRTEM, and c,d) FESEM images of Cu_2O films. A lattice spacing of 0.246 nm corresponds to the (111) plane of Cu_2O in (b).

and stability of TiO_2 NRs under air mass 1.5 global (AM 1.5G) make it a suitable photoanode to investigate the properties of different cathodes (Figure S1).[15b,16] The dark current–potential (*J*–*V*) curves for water splitting were measured in N_2-saturated 0.1 M $KHCO_3$ using a two-electrode configuration with TiO_2 NRs as working electrode (WE) and Pt, Cu, and Cu_2O cathodes as counter electrodes (CE), respectively (Figure 2a). The highest onset potential of dark *J*–*V* curves by the Cu_2O cathode indicated the highest reaction overpotential for HER on this surface. The PEC

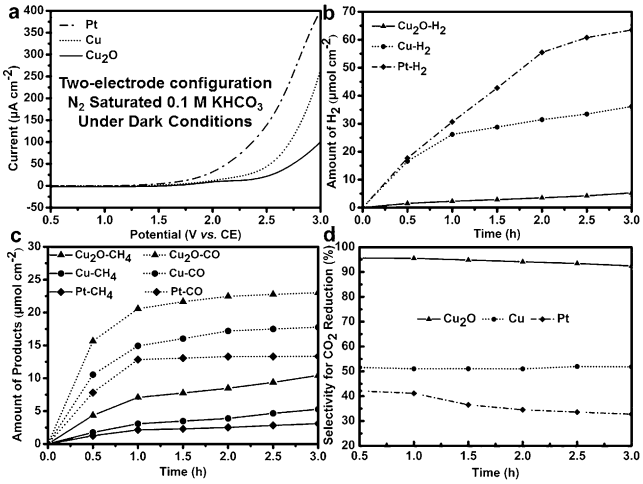

Figure 2. a) *J*–*V* curves using different cathodes measured in N_2-saturated 0.1 M $KHCO_3$ (pH 9.3) under dark conditions by two-electrode configuration with TiO_2 NRs as WE and different cathodes as CE. Amounts of b) H_2, c) CO, and CH_4 as a function of reaction time using TiO_2 NRs as WE, different cathodes as CE and saturated Ag/AgCl as the RE under 100 mW cm^{-2} AM 1.5G and 0.75 V vs. RHE. d) The calculated SCP by different cathodes as a function of reaction time. Experimental details and calculated methods can be found in the Supporting Information.

CO_2 reduction reactions were conducted in CO_2-saturated 0.1 M $KHCO_3$ (pH 6.9) using a typical three-electrode configuration with TiO_2 NRs as WE, saturated Ag/AgCl as reference electrode (RE), and Pt, Cu, and Cu_2O cathodes as CE, respectively (Figure S2). To compare with previous works, the PEC CO_2 reduction reactions were all conducted under 100 mW cm^{-2} AM 1.5G and a constant external bias of 0.75 V versus the reversible hydrogen electrode (RHE).[7] The reduction of CO_2 occurred on the surface of different cathodes and the main products were CO, CH_4, and H_2, with trace amounts of CH_3OH (Figure 2b and c), as summarized in Table 1. For the Cu_2O cathode, the amount of H_2 was the lowest, whereas the amounts of CO and CH_4 were the highest compared with Pt and Cu cathodes, which resulted in a high SCP of over 90% during the reaction (Figure 2d). The current density–time (*J*–*t*) curves for the Cu_2O dark cathode during the reaction are shown in Figure 3a. In addition, the *J*–*V* curves under AM 1.5G in 0.1 M $KHCO_3$-saturated by different kinds of gases could provide

Table 1: PEC CO_2 reduction products after the reaction for 3 hours with different electrodes under 100 mW cm^{-2} AM 1.5G.

Electrodes[a] (Working/Counter)	E[b] [V_{RHE}]	Average Current Density[c] [mA cm^{-2}]	Faradaic Efficiency[d] [%]					Sel. [%][e]
			CH_4	CO	CH_3OH	H_2	Total	
TiO_2 NRs/ Pt	0.75	1.37	15.86	17.05	0.11	65.07	98.09	33.66
TiO_2 NRs/ Cu	0.75	1.36	27.36	23.01	1.11	46.82	98.30	52.37
TiO_2 NRs/ Cu_2O	0.75	1.34	54.63	30.03	2.79	6.94	94.39	92.65
Cu_2O/ Pt	−0.1	0.71	35.62	19.01	0.34	31.43	86.40	63.62
TiO_2 NRs/ Cu_2O@TiO_2	0.75	1.24	22.72	30.89	1.44	41.61	96.66	56.95

[a] The working electrodes were under illumination and counter electrodes were shadowed during the reaction. [b] E: the external bias vs. RHE. [c] The average current densities were achieved by the integration over 3 h reaction. [d] The calculated methods for Faradaic efficiencies can be found in the Supporting Information. [e] Sel.: the selectivity towards carbonaceous products on an electron basis.

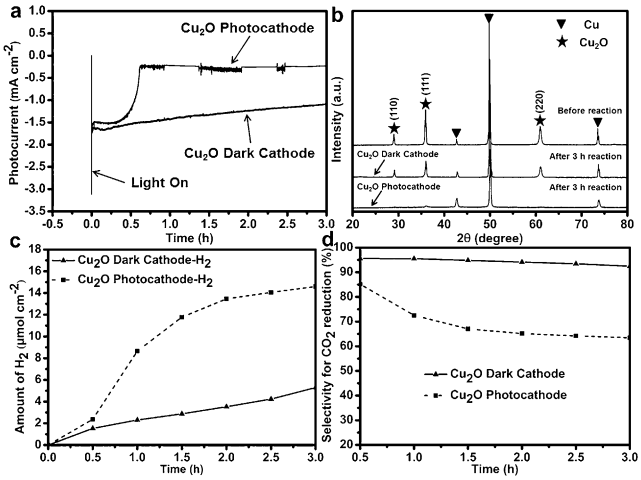

Figure 3. a) *J*–*t* curves during the reactions. b) XRD patterns of Cu_2O electrodes before and after the 3 h reactions. c) Amounts of H_2 and d) SCP as a function of the reaction time using different electrodes by three-electrode configuration in PEC CO_2 reduction.

more insights into the differences between Pt, Cu, and Cu_2O cathodes in PEC CO_2 reduction (Figure S3). It has been widely accepted that CO is the key intermediate during CO_2 reduction and can be further reduced to hydrocarbons and alcohols.[17] Therefore, the adsorption strength of CO on the electrode is critical to the final products. Ideally, the intermediates, such as CO, should be bound strongly enough to facilitate CO_2 reduction, but not so strongly that the intermediates are unreactive.[18] A comparison study between the Pt, Cu, and Cu_2O electrodes revealed that the CO adsorption on Pt surface is so strong that CO will occupy the active sites for CO_2 reduction (Figure S3). Thus, the majority of electrons will take part in HER and lead to a low yield of carbonaceous products on Pt.[17,19] The CO adsorption strength on Cu and Cu_2O is moderate and can be removed under N_2 atmosphere so that it can be further reduced into hydrocarbons. Therefore, the utilization of Cu_2O in PEC CO_2 reduction is of great importance for the efficient conversion of CO_2.

However, Cu_2O severely suffers from poor stability owing to corrosion. To investigate the performance of the Cu_2O photocathode in PEC CO_2 reduction, Cu_2O films were directly used as WE under illumination, with saturated Ag/AgCl as RE and a Pt foil as CE. Before the reaction, typical *J*–*V* curves of Cu_2O photocathode were acquired under AM 1.5G in CO_2-saturated 0.1 M $KHCO_3$ (Figure S4). To obtain a similar initial current value ($\approx 1.5\ mA\,cm^{-2}$) for the Cu_2O dark cathode and photocathode, the photo-assisted reaction was conducted under a potential of −0.1 V versus RHE. The reduction of CO_2 occurred on the surface of Cu_2O, and the comparison results are shown in Figure 3. The deactivation of the Cu_2O photocathode could be clearly observed during the reaction. The similar initial current values between the two situations indicated a similar amount of charges ($\approx 2.7\ C\,c^{-2}$ in the first 0.5 h) passed through the two electrodes. During the 3 h reaction, the current densities of Cu_2O photocathode remained stable for less than 0.5 h and decreased sharply. In contrast, only a slight reduction in the current densities was observed for the Cu_2O dark cathode (Figure 3a). X-ray diffraction (XRD) patterns of the Cu_2O films before and after the reactions showed that the characteristic peaks of Cu_2O completely disappeared after the 3 h reaction when it was directly used as photocathode, in notable contrast to the Cu_2O dark cathode (Figure 3b). The corrosion of the Cu_2O photocathode led to a higher H_2 evolution amount and lower SCP (Figure 3c and d, dash lines; the carbonaceous products over the Cu_2O photocathode are shown in Figure S5). However, the SCP remained above 90% during the 3 h reaction over the Cu_2O dark cathode (Figure 3d, solid line). In addition, there were many surface cracks on the Cu_2O photocathode films, and the surface profile was almost broken after 3 h illumination with external bias (Figure 1c,d and Figure S6a,b). In contrast, the surface morphological profile of Cu_2O dark cathode films remained unchanged, with no surface cracks after 3 h reaction (Figure 1c,d and Figure S6c,d). The excellent stability of the Cu_2O dark cathode in PEC CO_2 reduction was further demonstrated by a longer reaction time of 6 h (Figure S7). Therefore, using Cu_2O as a dark cathode in our system was an efficient way to maintain its stability and improve the SCP for PEC CO_2 reduction.

These results are somewhat unexpected and deserve further investigations because only Cu_2O with an excellent stability can result in a high SCP for CO_2 photoreduction. Considering the differences between these two situations, three factors that may lead to different Cu_2O stabilities are proposed and examined: the electrons ready for surface reactions, the photogenerated transient highly energetic electrons, and the photogenerated holes. First, electrons with different electric potentials will exhibit different powers to drive the reduction reaction and result in different Cu_2O corrosion rates. The average potential of electrons photogenerated by TiO_2 is lower than those by the Cu_2O photocathode owing to the lower conduction band edge of TiO_2. However, when electrons generated by TiO_2 were transferred to the Cu_2O dark cathode through an external circuit, their potential would be elevated by the higher external bias of 0.75 V versus RHE. Nevertheless, a lower external bias of −0.1 V versus RHE was applied on the Cu_2O photocathode, which could lead to the similar average potential of electrons between the Cu_2O photocathode and dark cathode. Meanwhile, the same kinds of products were generated on both Cu_2O cathodes, indicating that the electrons on both surfaces had similar potentials and enough driving force to reduce CO_2 into CO, CH_4, and CH_3OH. Additionally, the similar initial current densities over the Cu_2O photocathode and dark cathode indicated a similar amount of charges passed through the electrodes. Therefore, one may expect that the Cu_2O photocathode and dark cathode would exhibit similar stability under the experimental conditions. However, these two electrodes showed different stabilities, indicating that the reduction of Cu_2O by electrons is unlikely the main reason for its corrosion.

In contrast to the electrons ready for surface reactions mentioned above, the photogenerated transient electrons are highly energetic and hold a much higher reduction capability. There is a large number of photons with energy much higher

than the band gap energy of Cu_2O in the AM 1.5G spectrum. The transient electrons excited by these photons possess much higher potential levels than the conduction band edge of Cu_2O and a large driving force for reduction reactions. However, these photogenerated transient highly energetic electrons did not exist on the Cu_2O dark cathode, whose electrons came from the external circuit. Upon generation, the transient electrons will relax into lower states in the conduction band (usually the bottom) or interband trap states on a femtosecond time scale before they take part in redox reactions, which usually occur on a longer time scale.[17b,20] This can explain why these transient highly energetic electrons barely provide a higher reduction potential. To investigate the effects of highly energetic electrons, a Cu_2O film was electrodeposited on a FTO substrate to perform the stability tests. The *J*–*t* curves were measured at 0 V versus RHE in N_2-saturated 0.5 M Na_2SO_4 using the typical three-electrode configuration. The light source was AM 1.5G with/without cut-off filters (all the light intensity was adjusted to 100 mW cm^{-2}). With the cut-off filters, a large portion of highly energetic photons could be filtered out from AM 1.5G, however, the Cu_2O films did not exhibit better stability, as evidenced by the *J*–*t* curves (Figure 4a). Therefore, the photogenerated highly energetic electron is excluded as the main reason for Cu_2O corrosion.

Additionally, the most obvious differences between the Cu_2O photocathode and dark cathode in Figure 3 are the photogenerated holes. The Cu_2O photocathode harvested photons to generate both electrons and holes. However, the oxidative holes were hardly present in the Cu_2O dark cathode. It is known that the redox potentials for Cu_2O reduction (into Cu) and oxidation (into CuO) lie within its band gap,[10] which means that the oxidation of Cu_2O into CuO by holes could also lead to its deactivation. Wu et al. have found that the morphology changes from a dense structure to a network of leaf-like crystals with the transformation from Cu_2O to CuO play a critical role in the degradation of its photocurrent.[21] In this work, the back-side illumination, which generated electron–hole pairs near the back contact in contrast to front illumination, was utilized to investigate the difference in Cu_2O stability. For a photocathode, electrons are consumed at the photocathode/electrolyte interface, whereas the holes need to travel to the back contact and the counter electrode. Therefore, the travel distances of electrons and holes are much different between front and back illumination (Figure 4c).[22] Back illumination, in which the travel distance of electrons is much longer than that of holes, exhibited better Cu_2O stability than front illumination, as evidenced by *J*–*t* curves (Figure 4b), indicating that the holes may have more adverse effects on the stability of Cu_2O than electrons. Therefore, the shadowing of Cu_2O in this work to minimize the adverse effects of holes is a simple but efficient strategy to improve its stability and the SCP during the reaction.

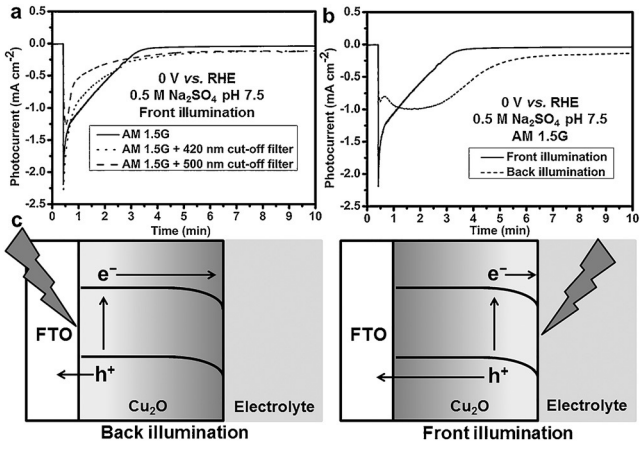

Figure 4. *J*–*t* curves of Cu_2O photocathode under a) different light sources and b) front and back illumination. The measurements were conducted at 0 V vs. RHE in N_2-saturated 0.5 M Na_2SO_4 using Cu_2O film as WE, saturated Ag/AgCl as RE and a Pt foil as CE. All of the light intensity was adjusted to 100 mW cm^{-2}. Under back illumination, the light intensity was measured behind a piece of bare FTO substrate. c) Diagram of the front and back illumination showing the different distances that electrons and holes have to travel.

It has been reported that the coating of protective layers (for example, TiO_2) on the surface of unstable electrodes can efficiently improve their stability.[23] In this work, TiO_2 was deposited on the Cu_2O electrode by atomic layer deposition (ALD) to suppress its corrosion. The as-prepared Cu_2O@TiO_2 dark cathode indeed exhibited better stability, but lower SCP than bare Cu_2O owing to the cover of surface active sites (Figure S8). Therefore, the use of Cu_2O as a dark cathode in this work could improve its stability and promote the exposure of active sites simultaneously for high SCP of CO_2 reduction. The calculated FEs and SCPs using different electrodes are shown in Table 1.

In summary, we have demonstrated a simple approach to achieve stable PEC CO_2 reduction with high FE and SCP by shadowing the Cu_2O electrode from illumination while exposing it to the electrolytes. Using Cu_2O as a dark cathode, FE of 87.45% and selectivity of 92.65% for all carbonaceous products were achieved at a low bias of 0.75 V versus RHE. Meanwhile, it was found that photogenerated holes may have more adverse effects on the Cu_2O stability than electrons, which led to the unexpectedly large differences of stability between the Cu_2O photocathode and dark cathode. It could be inferred from this study that properly designed photocatalytic systems, which can minimize the adverse effects of holes on Cu_2O, may be an efficient way to enhance its stability and further improve the selectivity for carbonaceous products in CO_2 photoreduction.

Acknowledgements

We acknowledge the National Science Foundation of China (U1463205, 21525626, 51302185), Specialized Research Fund for the Doctoral Program of Higher Education (20120032110024, 20130032120018), the Scientific Research Foundation for the Returned Overseas Chinese Scholars (MoE), and the Program of Introducing Talents of Discipline to Universities (B06006) for financial support.

Keywords: carbon dioxide reduction · cuprous oxide · photocatalysis · photoelectrochemistry · stability

How to cite: *Angew. Chem. Int. Ed.* **2016**, *55*, 8840 – 8845
Angew. Chem. **2016**, *128*, 8986 – 8991

[1] A. Goeppert, M. Czaun, J. P. Jones, G. K. Surya Prakash, G. A. Olah, *Chem. Soc. Rev.* **2014**, *43*, 7995 – 8048.
[2] a) M. Halmann, *Nature* **1978**, *275*, 115 – 116; b) X. Li, J. Wen, J. Low, Y. Fang, J. Yu, *Sci. China Mater.* **2014**, *57*, 70 – 100; c) S. Xie, Q. Zhang, G. Liu, Y. Wang, *Chem. Commun.* **2016**, *52*, 35 – 59; d) W. Tu, Y. Zhou, Z. Zou, *Adv. Mater.* **2014**, *26*, 4607 – 4626; e) J. L. White, M. F. Baruch, J. E. Pander Iii, Y. Hu, I. C. Fortmeyer, J. E. Park, T. Zhang, K. Liao, J. Gu, Y. Yan, T. W. Shaw, E. Abelev, A. B. Bocarsly, *Chem. Rev.* **2015**, *115*, 12888 – 12935.
[3] B. Kumar, M. Llorente, J. Froehlich, T. Dang, A. Sathrum, C. P. Kubiak, *Annu. Rev. Phys. Chem.* **2012**, *63*, 541 – 569.
[4] J. Hong, W. Zhang, J. Ren, R. Xu, *Anal. Methods* **2013**, *5*, 1086 – 1097.
[5] X. Chang, T. Wang, J. Gong, *Energy Environ. Sci.* **2016**, DOI: 10.1039/C6EE00383D.
[6] J. Ran, J. Zhang, J. Yu, M. Jaroniec, S. Z. Qiao, *Chem. Soc. Rev.* **2014**, *43*, 7787 – 7812.
[7] G. Magesh, E. S. Kim, H. J. Kang, M. Banu, J. Y. Kim, J. H. Kim, J. S. Lee, *J. Mater. Chem. A* **2014**, *2*, 2044 – 2049.
[8] a) G. Ghadimkhani, N. R. de Tacconi, W. Chanmanee, C. Janaky, K. Rajeshwar, *Chem. Commun.* **2013**, *49*, 1297 – 1299; b) K. Rajeshwar, N. R. de Tacconi, G. Ghadimkhani, W. Chanmanee, C. Janaky, *ChemPhysChem* **2013**, *14*, 2251 – 2259.
[9] Q. Zhai, S. Xie, W. Fan, Q. Zhang, Y. Wang, W. Deng, Y. Wang, *Angew. Chem. Int. Ed.* **2013**, *52*, 5776 – 5779; *Angew. Chem.* **2013**, *125*, 5888 – 5891.
[10] A. Paracchino, V. Laporte, K. Sivula, M. Gratzel, E. Thimsen, *Nat. Mater.* **2011**, *10*, 456 – 461.
[11] R. Wick, S. D. Tilley, *J. Phys. Chem. C* **2015**, *119*, 26243 – 26257.
[12] a) C. Li, T. Hisatomi, O. Watanabe, M. Nakabayashi, N. Shibata, K. Domen, J.-J. Delaunay, *Energy Environ. Sci.* **2015**, *8*, 1493 – 1500; b) M. Schreier, P. Gao, M. T. Mayer, J. Luo, T. Moehl, M. K. Nazeeruddin, S. D. Tilley, M. Grätzel, *Energy Environ. Sci.* **2015**, *8*, 855 – 861; c) T. Wang, Z. Luo, C. Li, J. Gong, *Chem. Soc. Rev.* **2014**, *43*, 7469 – 7484; d) T. Wang, J. Gong, *Angew. Chem. Int. Ed.* **2015**, *54*, 10718 – 10732; *Angew. Chem.* **2015**, *127*, 10866 – 10881.
[13] M. Schreier, J. Luo, P. Gao, T. Moehl, M. T. Mayer, M. Grätzel, *J. Am. Chem. Soc.* **2016**, *138*, 1938 – 1946.
[14] a) Y. J. Jang, J.-W. Jang, J. Lee, J. H. Kim, H. Kumagai, J. Lee, T. Minegishi, J. Kubota, K. Domen, J. S. Lee, *Energy Environ. Sci.* **2015**, *8*, 3597 – 3604; b) J.-W. Jang, S. Cho, G. Magesh, Y. J. Jang, J. Y. Kim, W. Y. Kim, J. K. Seo, S. Kim, K.-H. Lee, J. S. Lee, *Angew. Chem. Int. Ed.* **2014**, *53*, 5852 – 5857; *Angew. Chem.* **2014**, *126*, 5962 – 5967.
[15] a) X. Ba, L.-L. Yan, S. Huang, J. Yu, X.-J. Xia, Y. Yu, *J. Phys. Chem. C* **2014**, *118*, 24467 – 24478; b) I. S. Cho, Z. Chen, A. J. Forman, D. R. Kim, P. M. Rao, T. F. Jaramillo, X. Zheng, *Nano Lett.* **2011**, *11*, 4978 – 4984.
[16] B. Liu, E. S. Aydil, *J. Am. Chem. Soc.* **2009**, *131*, 3985 – 3990.
[17] a) M. Gattrell, N. Gupta, A. Co, *J. Electroanal. Chem.* **2006**, *594*, 1 – 19; b) S. N. Habisreutinger, L. Schmidt-Mende, J. K. Stolarczyk, *Angew. Chem. Int. Ed.* **2013**, *52*, 7372 – 7408; *Angew. Chem.* **2013**, *125*, 7516 – 7557.
[18] B. A. Rosen, A. Salehi-Khojin, M. R. Thorson, W. Zhu, D. T. Whipple, P. J. Kenis, R. I. Masel, *Science* **2011**, *334*, 643 – 644.
[19] Y. Hori, A. Murata, R. Takahashi, *J. Chem. Soc. Faraday Trans. 1* **1989**, *85*, 2309.
[20] D. P. Colombo, R. M. Bowman, *J. Phys. Chem.* **1996**, *100*, 18445 – 18449.
[21] L. Wu, L.-k. Tsui, N. Swami, G. Zangari, *J. Phys. Chem. C* **2010**, *114*, 11551 – 11556.
[22] Y. Liang, T. Tsubota, L. P. A. Mooij, R. van de Krol, *J. Phys. Chem. C* **2011**, *115*, 17594 – 17598.
[23] a) S. Hu, M. R. Shaner, J. A. Beardslee, M. Lichterman, B. S. Brunschwig, N. S. Lewis, *Science* **2014**, *344*, 1005 – 1009; b) B. Seger, T. Pedersen, A. B. Laursen, P. C. Vesborg, O. Hansen, I. Chorkendorff, *J. Am. Chem. Soc.* **2013**, *135*, 1057 – 1064.

Received: March 25, 2016
Revised: April 27, 2016
Published online: May 20, 2016

